Fusion Journal of Engineering and Sciences

Type of the Paper (Article)

Study on the Hydrodynamic Effects of Vegetation in Spur Dike Induced Flow

Sohail Iqbal [1*], Rizwan Haider [2], Muhammad Zubair Zafar Shah [3] Nadir Murtaza [4]

[1] Department of Civil Engineering, Faculty of Science and Technology, Tokyo University of Science, Chiba 278-8510, Japan.
[2] School of Infrastructure Engineering, Dalian University of Technology, Dalian 116024, China.
[3] Graduate School of Science and Engineering, Saitama University, 255 Shimo okubo, Sakura ku, Saitama shi, Saitama 338 8570, Japan.
[4] Department of Civil Engineering, University of Engineering and Technology Taxila, Taxila 47050, Pakistan.
* Correspondence: sohailsakhani147@gmail.com

Abstract

This study investigates the hydraulic influence of localized vegetation introduced upstream of a spur dike in a rectangular channel using a validated computational fluid dynamics (CFD) model. Two scenarios were simulated: one without vegetation and another with a rigid vegetative patch positioned upstream of the spur dike. Analysis focused on flow distributions to assess the impact of vegetation. Results showed that the vegetation considered resulted to a consistent reduction in flow velocity and wall shear stress along both channel banks. The vegetative resistance weakened recirculation zones, attenuated shear layers, and redistributed momentum across the flow domain. Additionally, the presence of vegetation modified the flow structure by promoting more uniform velocity gradients and dampening turbulence intensity near the bed and banks, especially around the spur dike nose. This altered hydrodynamic behavior contributed to a noticeable decline in erosive forces, particularly in zones vulnerable to scour. The simulation outcomes underscore the potential of strategically placed vegetation in reducing local scour and improving bank protection. These findings demonstrate that even limited vegetation placement can effectively reduce erosive forces and enhance flow stability around spur dikes. The study supports the use of targeted vegetation as a nature-based solution in hybrid river training strategies, contributing to sustainable river engineering and flood management practices.

Keywords: Spur dike; Vegetation–flow interaction; Computational fluid dynamics (CFD); Open channel flow.

1. Introduction

T Rivers are dynamic systems that constantly reshape their morphology due to the interaction between flow dynamics and the surrounding environment. The management of riverbanks and flow alignment is a fundamental aspect of hydraulic engineering, especially in regions vulnerable to erosion, sediment transport, and habitat degradation [1]. To control these processes and maintain channel stability, various structural and non-structural interventions have been implemented over time [2–4]. Among these, spur dikes (commonly named groynes) are widely utilized. Spur dikes are installed perpendicularly

or at some angle from the riverbank into the main flow [5,6]. Their primary purpose is to redirect the flow away from the banks, reduce local velocity, promote sediment deposition, and ultimately protect the riverbanks from erosion [7].

While spur dikes are effective in altering flow patterns and stabilizing banks, their interaction with the approaching flow introduces complex hydrodynamic phenomena. These include separation zones, recirculation regions, and increased turbulence around the tips and downstream faces of the structures. Such flow modifications can lead to scour near the spur dike bases and may influence the sediment dynamics within the channel [8,9]. Furthermore, the arrangement, spacing, and geometric properties of spur dikes significantly affect the extent of their influence on the river hydrodynamics. Although spur dikes is well established hydraulic structure in river engineering, their combined interaction with ecological elements such as vegetation is an area of growing interest, especially in the context of sustainable and nature-based river management [3,7].

Vegetation plays a critical role in riverine environments [10]. Riparian and aquatic plants provide hydraulic resistance, reduce near-bed velocity, and contribute to sediment stabilization. They also enhance ecological diversity and serve as natural barriers against erosion. In the context of engineering applications, the deliberate placement of vegetation in or near the flow zone has been considered a soft engineering technique that complements hard structures like spur dikes. The introduction of vegetation upstream or around spur dikes can attenuate incoming flow energy [11,12], reduce turbulence intensity, and thus potentially diminish local scour as shown in Fig. 1. However, the effectiveness of such measures depends heavily on the density, distribution, and placement of the vegetation relative to the hydraulic structures [13].

In most practical applications, vegetation is not installed uniformly along either riverbanks or around all spur dikes due to site-specific constraints, ecological zoning policies, or budgetary limitations. As a result, asymmetrical or localized vegetation patterns are common [14,15]. These asymmetric configurations lead to uneven resistance distributions across the channel, resulting in complex three-dimensional flow behavior. Such cases are less commonly studied in the literature, which tends to focus on symmetric or fully vegetated scenarios. Consequently, there is a need to investigate how localized vegetation influences flow patterns and turbulence structures, especially when installed only on both sides of the channel or around selected spur dikes.

Fig. 1 Vegetation around spur dike located at RMB of Head Baloki, Pakistan

Despite the recognized importance of vegetation interactions, quantitative understanding of how localized upstream vegetation alters three-dimensional flow characteristics around spur dikes remains limited [2]. In particular, the influence of partial vegetation on key hydrodynamic indicators such as mean velocity redistribution, turbulence, and wall shear stresses structures has not been systematically explored. Existing studies predominantly emphasize fully vegetated channels or uniformly distributed vegetation,

which may not adequately represent real river management practices. Addressing this limitation is essential for improving the design of combined hard and soft river training measures that balance hydraulic efficiency, erosion control, and ecological sustainability.

This study aims to address this knowledge gap by examining the hydrodynamic effects of vegetation introduced at a strategic location upstream of the first spur dike on the right bank of a straight open channel. In this configuration, spur dikes are symmetrically installed on both banks of the channel, but vegetation is only placed on the upstream approach of the first spur dike along the right bank. This design simulates a partially vegetated river training scenario, which is both realistic and practically relevant. The impact of such partial vegetation on the flow dynamics is assessed in comparison to a baseline case without any vegetation. This comparison allows for the evaluation of how localized vegetative resistance modifies flow structures.

2. Materials and Methods

2.1. Governing Equations

To describe turbulent flow behavior, the instantaneous Navier–Stokes equations are Reynolds-averaged, resulting in the Reynolds-Averaged Navier–Stokes (RANS) equations. For steady, incompressible flow conditions, these equations consist of a continuity equation that enforces mass conservation and a momentum equation that represents the balance of forces acting on the fluid. The averaging process introduces additional Reynolds stress terms associated with velocity fluctuations, which require turbulence closure modeling. The governing RANS continuity and momentum equations are therefore written as follows [16]:

$$\frac{\partial U_i}{\partial x_i} = 0 \tag{1}$$

$$\frac{\partial (U_i U_j)}{\partial x_j} = \frac{1}{\rho}\frac{\partial P}{\partial x_i} + \frac{\partial}{\partial x_j}\left(\nu \frac{\partial U_i}{\partial x_j} - \overline{u_i' u_j'}\right) \tag{2}$$

Where, U_i and u_i' denote the mean and fluctuating velocity components in the x_i direction, respectively. P is indicative of mean pressure; $u_i' u_j'$ symbolize the Reynolds stresses, and the latter remains open. The overbar notation represents Reynolds time-averaging of the corresponding instantaneous flow variable, separating the flow into mean and fluctuating components. Application of Reynolds decomposition to the Navier–Stokes equations introduce additional unknown terms, known as the Reynolds stresses, which arise from correlations between velocity fluctuations. Since these stresses cannot be directly determined from the averaged equations, a closure problem emerges and requires supplementary modeling assumptions to express the Reynolds stresses in terms of mean flow quantities. The most commonly adopted closure strategy is the Boussinesq eddy viscosity hypothesis, which assumes that turbulent momentum transfer can be represented analogously to molecular viscosity. Accordingly, the Reynolds stresses are modeled as being linearly proportional to the gradients of the mean velocity field through an eddy viscosity coefficient, thereby linking turbulence effects to the resolved mean flow and enabling solution of the Reynolds averaged governing equations.

$$-\overline{u_i' u_j'} = \nu_t^* \left(\frac{\partial U_i}{\partial x_j} + \frac{\partial U_j}{\partial x_i}\right) - \frac{2}{3} k \delta_{ij} \tag{3}$$

where, ν_t^* denotes the turbulent (eddy) kinematic viscosity, and $k = \frac{1}{2}\overline{u_i' u_j'}$; presents the turbulent kinetic energy (*TKE*), defined as half of the mean square of the velocity fluctuations. In the framework of the standard k-ε urbulence model, the eddy viscosity, ν_t^* is evaluated using the following relationship:

$$\nu_t^* = C\mu \frac{k^2}{\varepsilon} \tag{4}$$

where, ε represents the dissipation of the *TKE*, the model utilizes the transport equations that are given below for k and ε:

$$\frac{\partial(U_j k)}{\partial x_j} = \frac{\partial}{\partial x_j}\left[\left(\nu + \frac{\nu_t^*}{\sigma_k}\right)\frac{\partial k}{\partial x_j}\right] + \nu_t^*\left(\frac{\partial U_i}{\partial x_j} + \frac{\partial U_j}{\partial x_i}\right)\frac{\partial U_i}{\partial x_j} - \varepsilon \quad (5)$$

$$\frac{\partial(U_j \varepsilon)}{\partial x_j} = \frac{\partial}{\partial x_j}\left[\left(\nu + \frac{\nu_t^*}{\sigma_\varepsilon}\right)\frac{\partial \varepsilon}{\partial x_j}\right] + C_{\varepsilon\cdot 1}\frac{\varepsilon}{k}\nu_t^*\left(\frac{\partial U_i}{\partial x_j} + \frac{\partial U_j}{\partial x_i}\right)\frac{\partial U_i}{\partial x_j} - C_{\varepsilon\cdot 2}\frac{\varepsilon^2}{k} \quad (6)$$

The model constants adopted in the governing equations are $c_\mu = 0.09$; $\sigma_k = 1.00$; $\sigma_\varepsilon = 1.30$; $C_{\varepsilon\cdot 1} = 1.44$; $C_{\varepsilon\cdot 2} = 1.92$. These coefficients are fixed parameters in the standard k-ε turbulence model and were originally calibrated through extensive experimental observations covering a wide variety of turbulent flow conditions [17]. Within Equations (5) and (6), the transport of turbulent kinetic energy k nd its dissipation rate ε due to turbulent mixing is modeled using the gradient diffusion hypothesis. In this approach, the turbulent Prandtl numbers σ_k and σ_ε relate the effective diffusivities of k and ε to the eddy viscosity ν_t^*, thereby enabling representation of turbulent diffusion processes in analogy with molecular diffusion.

2.2. Experimental Conditions

To validate the computational model used in this study, results were compared against experimental data obtained from a previously published flume study conducted at Zhejiang University, China [18]. The referenced experiments were performed in a multifunctional straight rectangular flume located in the Jiangong Test Hall. The experimental flume has a length of 50 m, a width of 1.2 m, and a height of 1.4 m, as illustrated in Figure 2. The spur dikes used in the experiment were fabricated from 0.016 m thick plexiglass and had a height of 0.40 m. These dikes were mounted vertically on the sidewalls of the flume. Flow velocity measurements were carried out using an Acoustic Doppler Velocimeter (ADV), which offers a velocity measurement range from −0.3 m/s to 0.3 m/s with a precision of ±1.0 mm/s. The sampling frequency was set at 25 Hz, and for each observation point, velocity data were recorded over a 30-second duration to obtain statistically stable estimates of time-averaged velocity components and turbulence intensity. In addition, a wave height recorder (WHR) was installed for measuring water surface elevation.

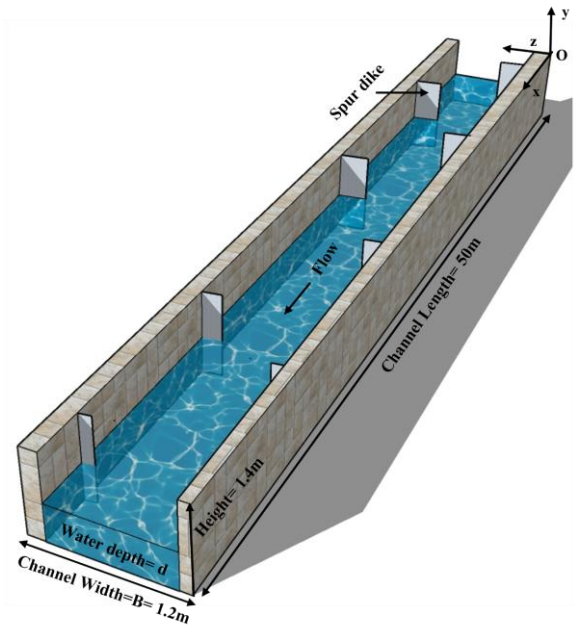

Fig. 2 Experimental conditions used Gu et al. [18]

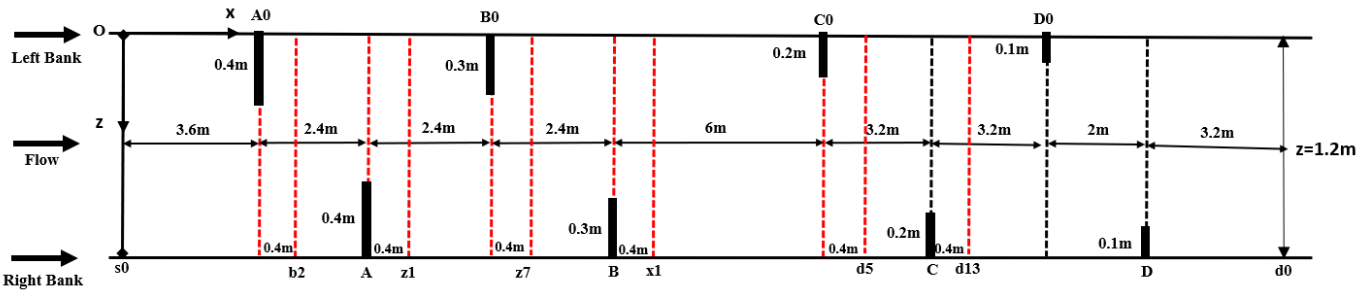

Fig. 3 Details of validation domain with different measuring locations

The spatial layout of the observing sections and measurement points is illustrated in Figure 3. Spur dikes were arranged at staggered cross-sections identified as A, A0, B, B0, C, C0, D, and D0. The flume inlet was located 3.6 m upstream from the first measurement cross-section (A0), and the outlet was positioned 3.2 m downstream from the last dike (D). Between sections A0 and D, a total of 57 vertical cross-sections were uniformly spaced at 0.4 m intervals, encompassing 607 observation points distributed throughout the test region. The coordinate system adopted in the experiment was defined as follows: the origin (O) was located at the flume bed; the X-axis was aligned with the main flow direction; the Y-axis was aligned vertically upward along the water depth; and the Z-axis was set along the axis of the spur dikes (transverse direction). Experiments were conducted under different hydraulic conditions for both non-submerged and submerged spur dike scenarios. Detailed hydraulic parameters and flow conditions are available in the source publication [18]. In the present study non-submerged cases are considered.

This experimental dataset was chosen for model validation due to its high spatial resolution, clear geometric documentation, and availability of three-dimensional velocity data, making it suitable for benchmarking numerical simulations of flow around multiple spur dikes in a controlled environment.

2.3. Modelling Setup

To reproduce the laboratory setup while preserving numerical efficiency, the numerical domain was reduced in length from the original 50 m to 28.4 m, as illustrated in Figure 3. This truncation was introduced to avoid an excessively large mesh size without compromising the essential geometric and flow characteristics of the setup described by Gu et al., [18]. All other structural dimensions (including flume width, dike spacing, and elevations) were kept identical to the experimental configuration to ensure meaningful validation. Given that the flow past spur dikes involves fully developed turbulence with strong shear layers and wake interactions, it was treated as fully turbulent. The standard k-ε turbulence model was choosen, owing to its robustness and efficiency in simulating high Reynolds number flows with separated regions and recirculation. Simulations were performed using the three-dimensional, pressure-based solver in ANSYS FLUENT. Pressure-velocity coupling was handled through the body force weighted scheme, which is suitable for free surface flows modeled under the rigid lid assumption. All transport equations (including those governing momentum, turbulent kinetic energy k, and its dissipation rate ε) were discretized using the first-order upwind scheme to ensure numerical stability and convergence.

A three-dimensional unstructured tetrahedral mesh was used to discretize the flow domain. Mesh refinement was applied to better capture high-gradient regions and complex flow features. A mesh independence study was carried out by systematically refining the mesh in both the spanwise and vertical directions. The results showed minimal

variation in velocity profiles, confirming the adequacy of the selected grid resolution. Therefore, the adopted mesh was retained for all simulations, and the results presented herein are mesh independent. The convergence threshold for all governing equations was set to 10^{-6}, ensuring reliable and consistent numerical outputs across the simulation domain.

2.4. Simulation Setup

The current study investigates the impact of localized vegetation on the hydrodynamics around a spur dike through two computational cases, illustrated in Figure 3. Both cases share identical computational domains, boundary conditions, meshing strategies, and numerical models; the only difference is the introduction of vegetation in one scenario. This approach allows for a controlled, isolated assessment of vegetation effects on flow behavior. Case A (Without vegetation) serves as the reference configuration and replicates the experimental domain used for model validation. It consists of a rectangular flume section containing an emergent spur dike mounted perpendicular to the right channel wall at cross-section A. The dike height is b=0.4 m, and the thickness is 0.04b. No vegetation is introduced in this case, and the flow is allowed to develop freely around the spur dike under unobstructed conditions as shown in Figure 3 (a). Case B (With vegetation) maintains all physical and numerical settings identical to Case A (including domain dimensions, boundary conditions, turbulence model, meshing strategy, and solver parameters) but includes a patch of rigid vegetation upstream of the first spur dike on the right bank. The vegetation occupies a streamwise length of 0.5b and is positioned immediately upstream of the dike, as shown in Figure 4 (b).

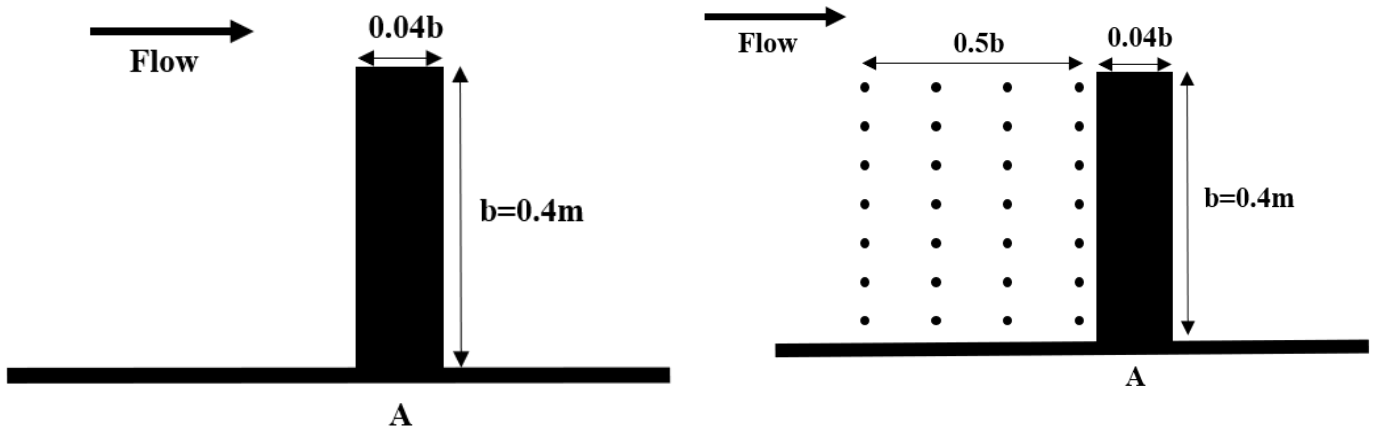

Fig. 4 Simulation cases, a. Without vegetation (Case A), and b. With vegetation (Case B)

3. Results

3.1. Validation

Computational models utilized in current study were validated using experimental data reported by Gu et al. [18] as shown in Figure 5. Specifically, validation was performed for a non-submerged spur dike scenario of Gu et al. [18], examining the velocity profiles at the monitoring cross-sections designated as b2, z1, z7, x1, d5, and d13. The comparison between computed results and experimental measurements demonstrated strong agreement, demonstrating the reliability of the computational model. The simulated velocity profiles consistently matched the measured velocities. The close match between the CFD results and the experimental data from Gu et al. [18] validates the

appropriateness and reliability of the computational methods employed. It indicates that the current CFD model is robust and appropriate for further hydrodynamic analyses and exploration of various spur dike configurations, including investigations involving vegetative impacts and altered geometric or hydraulic conditions.

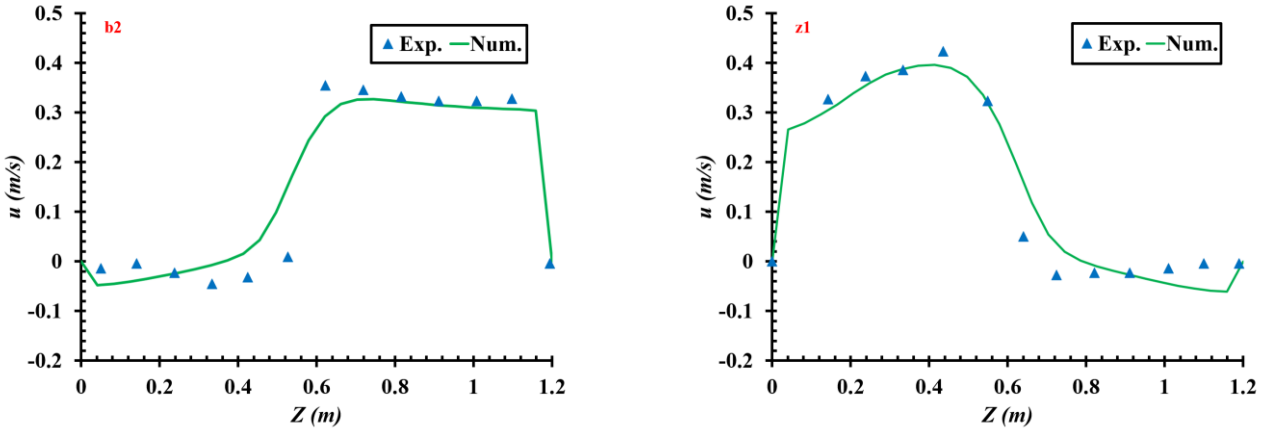

(a) (b)

Fig. 5 Comparison of numerical model with experimental results at different locations

A strong correspondence was observed at both monitoring locations (b2 and z1). The velocity profiles predicted by the simulation closely followed the measured distributions, indicating that the governing equations, boundary conditions, and turbulence representation were appropriately resolved. To quantitatively assess the predictive capability of the model, several statistical performance indices were employed, including the coefficient of determination (R^2), root mean square error (RMSE), normal¬ized root mean square error (NRMSE), normalized mean square error (NMSE), and mean absolute error (MAE) [19]. These metrics provide complementary information: R^2 evaluates the strength of correlation between measured and predicted values, whereas RMSE and MAE measure the magnitude of prediction errors, and NRMSE and NMSE enable comparison independent of scale. The mathematical expressions used to compute these statistical indicators are presented below.

$$\text{Root Mean Square Error (RMSE)} = \sqrt{\frac{1}{n}\sum_{i=0}^{n}\left(U_{Exp.} - U_{Num.}\right)^2} \quad (7)$$

$$\text{Normalized root mean square error (NRMSE)} = \frac{RMSE}{max(U_{Exp.}) - min(U_{Num.})} \quad (8)$$

$$\text{Normalized mean square error (NMSE)} = \frac{RMSE^2}{[max(U_{Exp.}) - min(U_{Exp.})].[max(U_{Num..}) - min(U_{Num..})]} \quad (9)$$

$$\text{Mean absolute error (MAE)} = \frac{1}{n}\sum_{i=0}^{n}\left|U_{Exp.} - U_{Num.}\right| \quad (10)$$

$$\text{Determination Coefficient } (R^2) = \left\{\frac{\sum_{i=0}^{n}[U_{Exp.} - \overline{U_{Exp.}}]}{\sqrt{\sum_{i=0}^{n}[U_{Exp.} - \overline{U_{Exp.}}]^2}} - \frac{\left[[U_{Num.} - \overline{U_{Num.}}\right]}{\sum_{i=0}^{n}[U_{Num.} - \overline{U_{Num.}}]^2}\right\}^2 \quad (11)$$

Table 1 presents a quantitative comparison between the numerically predicted and experimentally measured velocity data. The close correspondence observed across all cases verifies the predictive capability of the model and confirms that it provides a sound and dependable framework for subsequent analyses and extended applications.

Table 1 Comparison of numerical predictions with experimental measurements at multiple observation locations.

Cases	R^2	RMSE	NRMSE	NMSE	MAE
b2	0.9502	0.0327	0.0821	0.00133	0.0102
z1	0.980	0.0210	0.04	0.00051531	0.00734

3.2. Flow structure and velocity contours

Figure 6 displays the velocity magnitude contours for both simulation cases: (a) without vegetation (Case A) and (b) with vegetation (Case B). In Case A, where no vegetation is introduced, the flow accelerates significantly between spur dikes, producing high velocity zones and strong recirculation downstream of each structure. The high momentum regions are continuous and well-developed across the channel. In contrast, Case B, which includes a vegetation patch upstream of the first right-bank spur dike, shows a noticeable reduction in velocity across the channel. The vegetation introduces additional flow resistance, reducing the approach velocity before the first spur dike. As a result, the downstream velocity field becomes weaker, with less pronounced recirculation and lower momentum regions. This velocity reduction is not limited to the immediate area near the vegetation but extends downstream, influencing the entire dike field including left bank. Overall, the inclusion of localized vegetation in Case B leads to a general reduction in flow velocity throughout the channel, demonstrating its potential in dissipating flow energy and modifying dike-induced flow structures.

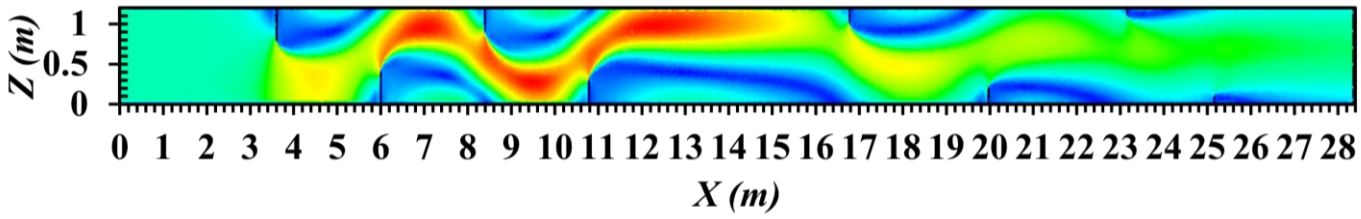

(a)

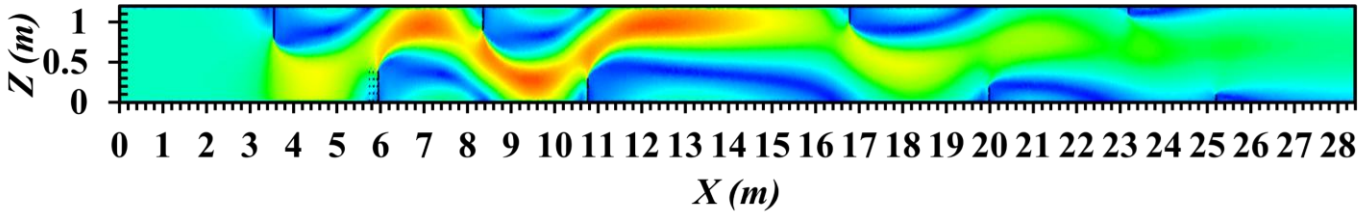

(b)

Fig. 6 Velocity contours, a. Without vegetation (Case A), and b. With vegetation (Case B)

3.3. Wall shear stress distribution

Figure 7 presents the wall shear stress distributions along the right bank (Figure 6a) and left bank (Figure 6b) for both simulation cases. In Case A (without vegetation), higher wall shear stress values are observed, particularly along the right bank near the spur dikes, with values peaking around 0.4 Pa. These peaks correspond to regions of high near-wall velocity gradients and are indicative of strong erosive potential. In Case B (with vegetation), a consistent reduction in wall shear stress is observed along both the right and left banks. On the right bank, this reduction is attributed directly to the upstream vegetation, which dampens the incoming flow and reduces the wall velocity gradient [20]. Interestingly, even on the left bank (which was not vegetated) the shear stress values are lower in Case B than in Case A. This suggests that the vegetation-induced momentum loss on the right bank causes redistribution of the flow field, resulting in less aggressive wall interaction across the channel. These results indicate that vegetation not only protects the immediate region of installation but also contributes to an overall reduction in wall-bound stress throughout the domain.

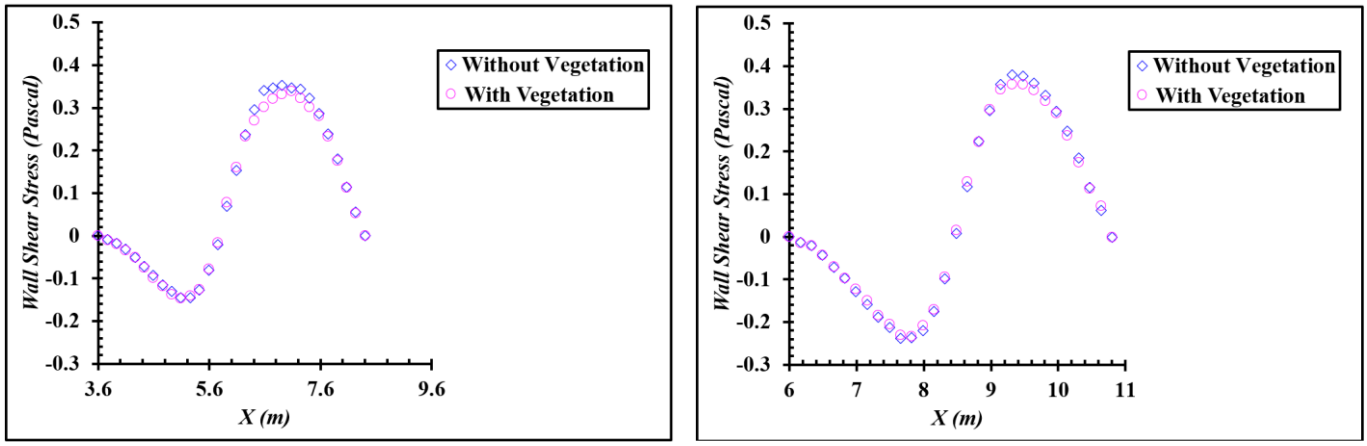

(a) (b)

Fig. 7 Wall shear stresses, a. Right bank, and b. Left bank

4. Discussion

The current study's results, (a channel-wide reduction in velocity magnitude, weakened recirculation, and lower wall shear stress on both banks when a localized, rigid vegetative patch is placed upstream of the first spur dike) are broadly consistent with prior experimental and numerical literature on vegetation flow structure interactions.

The observed damping of approach flow and attenuation of shear layers accord with the classical view that vegetation increases hydraulic resistance, reduces near-bed velocity, and mitigates erosive capacity (e.g., Hickin's synthesis on vegetation–channel dynamics) [20]. In our simulations, these effects extend beyond the vegetated bank and persist downstream across the spur-dike field. An outcome compatible with momentum redistribution processes described in earlier morphodynamical discussions of vegetated banks [21,22]. The reduction in wall shear stress along both banks is also aligned with findings from previous studies where vegetated surfaces enhance erosion resistance by dissipating near-wall stresses [23–25].

Moreover, compared with studies that focus on hydrodynamics around spur dikes without vegetation, our baseline patterns (Case A) reproduce the well-known acceleration between dikes and recirculation in their lee regions, as documented in CFD validations for spur-dike groups [18] and in recent multi-dike layout analyses [8]. Against that baseline, adding localized vegetation (Case B) yields a measurable weakening of those canonical features, consistent with recent computational works that embed vegetation elements near spur dikes and report reduced core velocities, suppressed turbulence production, and smaller recirculation cells [2,19]. Notably, Iqbal et al. [2] examined partially vs fully vegetated submerged spur dikes and similarly reported turbulence/velocity suppression with vegetation; our contribution complemented that line of evidence by showing that even asymmetric, localized vegetation upstream of an emerged spur dike can deliver comparable hydraulic benefits. Hence, relative to structural countermeasures that modify dike heads or add pile arrays to reshape the local flow (e.g., combined-head spur dikes [3], grouped piles near impermeable spur dikes [19], or submerged pile designs around emerged dikes [26]), the present results highlight a nature-based lever that achieves analogous hydraulic objectives (reducing approach momentum and stress hotspots) without altering the hard structure itself. This supports hybrid river-training structures in which selective vegetation placement is combined with hard measures to minimize erosive forcing while maintaining conveyance [1,3,7].

For design and maintenance, strategically placing compact vegetative patches upstream of the first spur dike on a vulnerable bank can (i) pre-condition the approach flow,

(ii) weaken shear layers at the dike nose, and (iii) reduce wall-bound stresses along both banks downstream, useful where continuous bankline planting is infeasible due to budget, zoning, or navigation constraints [13]. Such targeted patches are especially attractive as modular, low-cost additions to existing hard structures. Limitations and outlook. As with many hydraulic studies, our present analysis isolates rigid, emergent vegetation and does not yet couple sediment transport or bank erodibility. Prior work indicates that vegetation and sediment feedback can further amplify stabilization [20,27]; incorporating graded stem density, flexibility, and seasonality, alongside morpho dynamics, is a logical next step. Extending to oblique flows, compound channels, and field-scale heterogeneity would also help with site-specific guidelines.

5. Conclusions

This study employed a validated CFD model to analyze the hydraulic effects of introducing localized vegetation upstream of the spur dike in an open channel. The objective was to evaluate how rigid emergent vegetation influences flow characteristics, particularly velocity distribution and wall shear stress, by comparing configurations with and without vegetation. The results clearly showed that,

- The consideration of vegetation led to a reduction in flow velocity across the entire channel, not only in the immediate vicinity of the vegetation but also downstream throughout the spur dike field. The vegetation introduced additional resistance to the flow, decreasing the approach velocity, weakening recirculation zones, and lowering overall momentum in the channel.
- A consistent reduction in wall shear stress was observed along both the right and left banks in the presence of vegetation. This decrease indicates that localized vegetation placement contributes to mitigating erosive forces near the walls, even when applied in a limited region. The decline in wall shear stress on both sides of the channel highlights the broader hydraulic impact of vegetative resistance and suggests a redistribution of flow momentum across the section.

These findings demonstrate that even a small, localized application of vegetation can significantly influence flow behavior around spur dikes. By reducing both velocity and wall shear stress along both banks, vegetation enhances hydraulic stability and reduces the risk of local scour. This supports the implementation of targeted vegetation as a practical, nature-based component within hybrid river training systems. Future work should investigate the effects of varying vegetation densities, stem properties, and spatial layouts, as well as extend the modeling framework to include sediment transport and morphological evolution for evaluating long-term channel responses.

Author Contributions: Conceptualization, S.I., R.H. and N.M.; methodology, M.Z.Z.S. and R.H.; software, S.I. and R.H.; resources, R.H., M.Z.Z.S., and S.I.; writing—original draft preparation, S.I and N.M.; writing—review and editing, S.I., R.Z and M.Z.Z.S All authors have read and agreed to the published version of the manuscript

Funding: This research received no external funding.

Data Availability Statement: The data presented in this study are available upon request from the author

Conflicts of Interest: The authors declare no conflicts of interest.

References

1. H. Habersack, T. Hein, A. Stanica, I. Liska, R. Mair, E. Jäger, C. Hauer, C. Bradley, Challenges of river basin management: Current status of, and prospects for, the River Danube from a river engineering perspective, Science of the Total Environment 543 (2016) 828–845. https://doi.org/10.1016/j.scitotenv.2015.10.123
2. S. Iqbal, R. Haider, G.A. Pasha, L. Zhao, F.M. Abbas, N. Anjum, N. Murtaza, Z. Abbas, Numerical investigation of flow around partially and fully vegetated submerged spur dike, Water (Basel). 17 (2025) 435. https://doi.org/10.3390/w17030435
3. S. Iqbal, G.A. Pasha, U. Ghani, A. Ahmed, R. Farooq, R. Haider, Investigation of Flow Dynamics Around a Combination of Different Head Shapes of Spur Dikes, Tehnicki Vjesnik 29 (2022) 2111–2120. https://doi.org/10.17559/TV-20211230094323.
4. M. Asghar, G.A. Pasha, U. Ghani, S. Iqbal, M.S. Jameel, Investigating multiple debris impact load and role of vegetation in protection of house model during floods, in: 2nd Conference on Sustainability in Civil Engineering, 2020.
5. A. Kumar, C.S.P. Ojha, Review on the Field Applications of River Training Structures for River Bank Protection, in: The Ganga River Basin: A Hydrometeorological Approach, Springer, 2021: pp. 115–133. https://doi.org/10.1007/978-3-030-60869-9_8
6. Teraguchi, H., Nakagawa H., Nakgawa, H., Baba, Y., (2010) Morphological Changes induced by River Training Structures : Bandal-like structures and Groins. Annual Report of Disaster Prevention Research Institute, Kyoto University., No. 53 B
7. S. Iqbal, N. Tanaka, Hydraulic performance assessment of various submerged pile designs around an emerged dike, Water Science and Engineering (2024). https://doi.org/10.1016/j.wse.2024.02.002
8. R. Haider, S. Iqbal, F.M. Abbas, A. Fakhar, CFD analysis of flow dynamics around the series of dikes with alternative length layout, Natural Hazards 121 (2025) 8241–8260. https://doi.org/10.1007/s11069-025-07117-2
9. H.K. Yeo, J.G. Kang, S.J. Kim, An experimental study on tip velocity and downstream recirculation zone of single groynes of permeability change, KSCE Journal of Civil Engineering 9 (2005) 29–38. https://doi.org/10.1007/BF02829094
10. F.M. Abbas, Amina, G.A. Pasha, S. Iqbal, N. Anjum, M. Shahid, M. Iqbal, K. Mehmood, M.J. Butt, R. Haider, The Role of Angled Vegetation in Modifying Hydrodynamic Properties Around Dike, Ecohydrology 18 (2025) e70064. https://doi.org/10.1002/eco.70064
11. C. Wang, S. Zheng, P. Wang, J. Hou, Interactions between vegetation, water flow and sediment transport: A review, Journal of Hydrodynamics 27 (2015) 24–37. https://doi.org/10.1016/S1001-6058(15)60453-X
12. J. Aberle, J. Järvelä, Flow resistance of emergent rigid and flexible floodplain vegetation, Journal of Hydraulic Research 51 (2013) 33–45. https://doi.org/10.1080/00221686.2012.754795
13. M.A. McCarthy, K.M. Parris, R. Van Der Ree, M.J. McDonnell, M.A. Burgman, N.S.G. Williams, N. McLean, M.J. Harper, R. Meyer, A. Hahs, The habitat hectares approach to vegetation assessment: an evaluation and suggestions for improvement, Ecological Management & Restoration 5 (2004) 24–27. https://doi.org/10.1111/j.1442-8903.2004.00173.x
14. E.M. Follett, H.M. Nepf, Sediment patterns near a model patch of reedy emergent vegetation, Geomorphology 179 (2012) 141–151. https://doi.org/10.1016/j.geomorph.2012.08.006
15. O. Yagci, V.S. Özgur Kirca, V. Kitsikoudis, C.A.M.E. Wilson, M.F. Celik, C. Sertkan, Experimental study on influence of different patterns of an emergent vegetation patch on the flow field and scour/deposition processes in the wake region, Water Resour. Res. 60 (2024) e2023WR034978. https://doi.org/10.1029/2023WR034978
16. Y. Cheng, F.S. Lien, E. Yee, R. Sinclair, A comparison of large Eddy simulations with a standard k−ε Reynolds-averaged Navier–Stokes model for the prediction of a fully developed turbulent flow over a matrix of cubes, Journal of Wind Engineering and Industrial Aerodynamics 91 (2003) 1301–1328. https://doi.org/10.1016/j.jweia.2003.08.001
17. U. Manual, ANSYS FLUENT 12.0, Theory Guide 67 (2009).
18. Z. Gu, X. Cao, Y. Jiao, W.-Z. Lu, Appropriate CFD models for simulating flow around spur dike group along urban riverways, Water Resources Management 30 (2016) 4559–4570. https://doi.org/10.1007/s11269-016-1436-1
19. S. Iqbal, M. Siddique, A. Hamza, N. Murtaza, G.A. Pasha, Computational analysis of fluid dynamics in open channel with the vegetated spur dike, Innovative Infrastructure Solutions 9 (2024). https://doi.org/10.1007/s41062-024-01636-w
20. E.J. Hickin, Vegetation and river channel dynamics, Canadian Geographer/Le Géographe Canadien 28 (1984) 111–126.

21. C. Camporeale, E. Perucca, L. Ridolfi, A.M. Gurnell, Modeling the interactions between river morphodynamics and riparian vegetation, Reviews of Geophysics 51 (2013) 379–414. https://doi.org/10.1002/rog.20014
22. K. Shiono, M. Takeda, K. Yang, Y. Sugihara, T. Ishigaki, Modeling of vegetated rivers for inbank and overbank flows, in: Proceedings of the International Conference on Fluvial Hydraulics: River Flow, September 5–7, San Jose, Costa Rica, 2012: pp. 263–269.
23. A. Molinas, K. Kheireldin, B. Wu, Shear stress around vertical wall abutments, Journal of Hydraulic Engineering 124 (1998) 822–830. https://doi.org/10.1061/(ASCE)0733-9429(1998)124:8(822)
24. H.M. Nepf, E.R. Vivoni, Flow structure in depth-limited, vegetated flow, J. Geophys. Res. Oceans 105 (2000) 28547–28557. https://doi.org/10.1029/2000JC900145
25. D. Naot, I. Nezu, H. Nakagawa, Hydrodynamic Behavior of Partly Vegetated Open Channels, Journal of Hydraulic Engineering 122 (1996) 625–633. https://doi.org/10.1061/(asce)0733-9429(1996)122:11(625)
26. R. Haider, D. Qiao, X. Wang, J. Yan, D. Ning, Role of Grouped Piles on Flow Characteristics Around Impermeable Spur Dike, International Journal of Civil Engineering 3 (2022). https://doi.org/10.1007/s40999-022-00706-3
27. B. Scheres, H. Schüttrumpf, Investigating the erosion resistance of different vegetated surfaces for ecological enhancement of sea dikes, J. Mar. Sci. Eng. 8 (2020) 519. https://doi.org/10.3390/jmse8070519